

# Stochastic simulation of chemical exchange in two dimensional infrared spectroscopy

František Šanda <sup>\*†</sup> and Shaul Mukamel <sup>\*</sup>

*\* Department of Chemistry,  
University of California,  
Irvine, CA 92697-2025*

*† Charles University,  
Faculty of Mathematics and Physics,  
Institute of Physics,  
Ke Karlovu 5, Prague,  
121 16 The Czech Republic*

(Dated: August 13, 2018)

## Abstract

The stochastic Liouville equations are employed to investigate the combined signatures of chemical exchange (two-state-jump) and spectral diffusion (coupling to an overdamped Brownian oscillator) in the coherent response of an anharmonic vibration to three femtosecond infrared pulses. Simulations reproduce the main features recently observed in the OD stretch of phenol in benzene.

E-mail: smukamel@uci.edu

## I. INTRODUCTION

Recent experiments had demonstrated that two-dimensional infrared (2D IR) lineshapes can probe the picosecond dynamics of chemical exchange by observing coherence transfer in molecular vibrations through time-dependent spectral jumps<sup>1,2,3</sup>. This spectroscopic technique<sup>4,5,6</sup> is an optical analogue of 2D NMR commonly used to study slower (ms) chemical exchange processes<sup>7,8,9,10</sup>. In this three-pulse experiment (Fig 1) the first pulse creates a vibrational coherence, whose evolution (free induction decay) during the first interval  $t_1$  is related to the absorption lineshape by a Fourier transform. During the second interval  $t_2$  the vibrational frequency changes by complexation with the solvent. Finally vibrational coherence is again created by the third pulse and detected during the third interval  $t_3$ . The correlations of the lineshapes in the first and the third intervals provide information on chemical exchange taking place during the second interval.

One experiment<sup>1</sup> looked at the OD stretching mode of phenol in benzene whose frequency changes between  $2665\text{cm}^{-1}$  (free) and  $2631\text{cm}^{-1}$  (complexed). The 2D lineshapes monitor the dynamics of complex formation and dissociation<sup>1</sup>. For short delays ( $t_2 \sim 100\text{fs}$ ) two diagonal peaks broadened by spectral diffusion were observed at the linear-absorption frequencies. Off-diagonal cross-peaks are induced by chemical exchange for longer times ( $\sim 10\text{ps}$ ). Similar effects were seen in the overtone region. The rate constants for complexation were directly obtained from the peak kinetics.

Similar hydrogen-bonding dynamics were also reported for the CN stretch of acetonitrile in methanol<sup>3</sup>. The relative intensity of the two peaks attributed to free and hydrogen-bonded CN shows strong temperature dependence. The reaction coordinate profile in both ground and excited vibrational states was found to be very similar. The weak variation of the chemical exchange rates with changes in the vibrational state justifies the application of stochastic chemical exchange models<sup>11</sup> for vibration frequency fluctuations.

In this paper we use the stochastic Liouville equations (SLE) to simulate the effects of chemical exchange<sup>12,13,14</sup> and spectral diffusion in 2D lineshapes of an anharmonic vibration. This formalism was recently applied to model the signatures of conformational fluctuations in trialanine in water<sup>15</sup> using a Brownian oscillator coordinate model of fluctuations. The SLE were also used to compare the Brownian oscillator and the four-state-jump model of hydrogen bonding fluctuation on the photon echo of the OH stretch of HOD in DOD<sup>16</sup>.

In section II we introduce the anharmonic vibrational Hamiltonian subjected to fluctuations due to a two-state chemical-exchange and a Brownian oscillator coordinate. In the two state jump (TSJ) model of Kubo and Anderson<sup>7,17,18,19,20</sup> bath-assisted (incoherent) chemical exchange is described by kinetic equations. The model shows several distinct dynamical regimes depending on the motional narrowing parameter (ratio of the frequency shift and relaxation rate). Spectral diffusion<sup>1</sup> is incorporated by coupling to an overdamped Brownian oscillator coordinate<sup>21</sup>. The 2D IR signals are defined in section III. The stochastic Liouville equation for the TSJ model is introduced in section IV and the 2D IR signals are calculated for the limiting cases of slow and fast fluctuations and for short and long-time delays between pulses. The combined effect of spectral diffusion and TSJ is presented and analyzed in section V. All lineshape regimes observed in<sup>1</sup> are qualitatively reproduced.

## II. THE MODEL

We consider a single anharmonic vibrational mode described by the Hamiltonian:

$$H = \hbar\Omega B^\dagger B + \hbar\frac{\Delta}{2} B^\dagger B^\dagger B B \quad (1)$$

where  $B^\dagger$  ( $B$ ) are boson creation (annihilation) operators ( $[B, B^\dagger] = 1$ ). Both frequency ( $\Omega$ ) and anharmonicity ( $\Delta$ ) are subjected to fluctuations described by

$$\begin{aligned} \Omega &= \Omega_0 + \Omega_1\sigma_z + \Omega_2Q + \Omega_3\sigma_zQ, \\ \Delta &= \Delta_0 + \Delta_1\sigma_z + \Delta_2Q + \Delta_3\sigma_zQ. \end{aligned} \quad (2)$$

$\Omega_0$  and  $\Delta_0$  are the average values.  $\Omega_1$  and  $\Delta_1$  describe stochastic frequency modulation by chemical exchange represented by the TSJ model<sup>17,18</sup> (state up  $u$  ( $\sigma_z = 1$ ) and down  $d$  ( $\sigma_z = -1$ )).  $\sigma_z$  is the Pauli spin matrix .

$$\sigma_z = \begin{pmatrix} 1 & 0 \\ 0 & -1 \end{pmatrix}$$

$Q$  is an overdamped Brownian oscillator (BO) coordinate causing spectral diffusion and coupled to the vibration through the parameters  $\Omega_2$ , and  $\Delta_2$ .  $\Omega_3$ , and  $\Delta_3$  allow the spectral diffusion to have a different magnitude in the two spin states. We shall divide hamiltonian (Eq. (1)) into three parts  $H = H_{SV} + H_{QV} + H_{QS\dot{V}}$  where  $H_{SV}$  includes the first two (spin-vibration) terms in Eq.(2) which do not depends on  $Q$ , and  $H_{QV}, H_{QS\dot{V}}$  include the third

and fourth terms in Eq.(2) respectively. The dipole interaction with the electric field  $E(t)$  is<sup>22</sup>

$$H_{int} = -\mu E(t) (B^\dagger + B) \quad (3)$$

Three vibrational levels (Fig 1) are accessible in a three-pulse experiment: the ground state  $|g\rangle$ , the first excited  $|e\rangle \equiv B^\dagger|g\rangle$  and the doubly excited  $|f\rangle \equiv (1/\sqrt{2})B^\dagger B^\dagger|g\rangle$  state, with energies 0,  $\Omega$  and  $\Omega + \Delta$  respectively. The corresponding 9-component Liouville space basis set for the density matrix is denoted  $|\nu\nu'\rangle \equiv |\nu\rangle\langle\nu'|$ ;  $\nu, \nu' = e, f, g$ . The dipole moment matrix elements are  $\mu_{eg} = \mu$ ;  $\mu_{ef} = \sqrt{2}\mu$ .

### III. THE THIRD ORDER RESPONSE AND 2D SIGNALS

We consider an impulsive four wave mixing process whereby the vibrational mode (Eq.(1)) interacts with three impulsive optical pulses with intervals  $t_1, t_2$ , and calculate the response at  $t_3$  (see Fig 1). Each interaction with the field can create or annihilate one vibrational quantum at a time (Eq(3)). The equilibrium distribution is

$$|\rho(0)\rangle\rangle_{\mathcal{H}} = |\rho(0)\rangle\rangle_S |0\rangle_Q |gg\rangle \quad (4)$$

where  $|\rho(0)\rangle\rangle_S$  is equilibrium spin state and  $|0\rangle_Q$  equilibrium Brownian coordinate density given by Eq. (D1). The space  $\mathcal{H}$  is a direct product of the vibrational, spin and BO space.

The polarization generated in this experiment is described by the third order response function<sup>4</sup>

$$S^{(3)}(t_1, t_2, t_3) = \left(\frac{i}{\hbar}\right)^3 \theta(t_1)\theta(t_2)\theta(t_3) \langle\langle I | \mu^{(-)} \mathcal{G}(t_3) \mu^{(-)} \mathcal{G}(t_2) \mu^{(-)} \mathcal{G}(t_1) \mu^{(-)} | \rho(0) \rangle\rangle_{\mathcal{H}} \quad (5)$$

where  $\mu^{(-)}\xi \equiv \mu[B + B^\dagger, \xi]$ . Summing over final states is represented by  $\langle\langle I |_{\mathcal{H}} \equiv \langle I |_S \langle 0 |_Q Tr$  where  $\langle I |_S \equiv (1, 1)$ ,  $\langle 0 |_Q \equiv \int dQ$  and tracing is over the vibrational degrees of freedom  $Tr = \langle\langle gg | + \langle\langle ee | + \langle\langle ff |$ . The time evolution between pulses is described by the Green's function  $\mathcal{G}(t)$  of the SLE defined in the space  $\mathcal{H}$ .

The Liouville space state cannot change between pulses, so that Green functions are block-diagonal. The response functions can be separated into six contributions from different Liouville space pathways.

$$R_i(t_3, t_2, t_1) \equiv \langle I | \mathcal{G}_{eg, eg}(t_3) \mathcal{G}_{ee, ee}(t_2) \mathcal{G}_{eg, eg}(t_1) | \rho(0) \rangle\rangle_{QS}$$

$$\begin{aligned}
R_{ii}(t_3, t_2, t_1) &\equiv \langle I | \mathcal{G}_{eg, eg}(t_3) \mathcal{G}_{ee, ee}(t_2) \mathcal{G}_{ge, ge}(t_1) | \rho(0) \rangle_{QS} \\
R_{iii}(t_3, t_2, t_1) &\equiv \langle I | \mathcal{G}_{eg, eg}(t_3) \mathcal{G}_{gg, gg}(t_2) \mathcal{G}_{eg, eg}(t_1) | \rho(0) \rangle_{QS} \\
R_{iv}(t_3, t_2, t_1) &\equiv \langle I | \mathcal{G}_{eg, eg}(t_3) \mathcal{G}_{gg, gg}(t_2) \mathcal{G}_{ge, ge}(t_1) | \rho(0) \rangle_{QS} \\
R_v(t_3, t_2, t_1) &\equiv -\langle I | \mathcal{G}_{fe, fe}(t_3) \mathcal{G}_{ee, ee}(t_2) \mathcal{G}_{eg, eg}(t_1) | \rho(0) \rangle_{QS} \\
R_{vi}(t_3, t_2, t_1) &\equiv -\langle I | \mathcal{G}_{fe, fe}(t_3) \mathcal{G}_{ee, ee}(t_2) \mathcal{G}_{ge, ge}(t_1) | \rho(0) \rangle_{QS}
\end{aligned} \tag{6}$$

These may be graphically represented by the Feynman diagrams<sup>23</sup> given in Fig 1. For the stochastic models of frequency fluctuations considered here we have  $R_i = R_{iii}$  and  $R_{ii} = R_{iv}$ , so that we only need to consider four independent pathways<sup>23</sup>. The Green's function matrix elements  $\mathcal{G}_{fe, fe}(t_3)$  etc. are now matrices in the joint spin and BO space.

We shall display the signal using the mixed time-frequency representation

$$R_\alpha(\omega_3, t_2, \omega_1) \equiv \int_0^\infty \int_0^\infty \exp(i\omega_1 t_1 + i\omega_3 t_3) R_\alpha(t_3, t_2, t_1) dt_3 dt_1 \tag{7}$$

Eq. (6) then reads

$$R_i(\omega_3, t_2, \omega_1) = \langle I | \mathcal{G}_{eg, eg}(\omega_3) \mathcal{G}_{ee, ee}(t_2) \mathcal{G}_{eg, eg}(\omega_1) | \rho(0) \rangle_{QS};$$

and similarly for other pathways, where

$$\mathcal{G}(\omega) \equiv \int_0^\infty \mathcal{G}(t) e^{i\omega t} dt$$

We consider the coherent nonlinear signals generated in the  $\mathbf{k}_I = -\mathbf{k}_1 + \mathbf{k}_2 + \mathbf{k}_3$  and  $\mathbf{k}_{II} = \mathbf{k}_1 - \mathbf{k}_2 + \mathbf{k}_3$  phase-matching directions. Invoking the rotating wave approximation the  $\mathbf{k}_I$  (photon echo) signal is<sup>23</sup>

$$S_I(\omega_3, t_2, \omega_1) = \left(\frac{i}{\hbar}\right)^3 \left\{ \mu_{eg}^4 [R_{ii}(\omega_3, t_2, \omega_1) + R_{iv}(\omega_3, t_2, \omega_1)] + \mu_{eg}^2 \mu_{ef}^2 R_{vi}(\omega_3, t_2, \omega_1) \right\} \tag{8}$$

and for the  $\mathbf{k}_{II}$  signal we have

$$S_{II}(\omega_3, t_2, \omega_1) = \left(\frac{i}{\hbar}\right)^3 \left\{ \mu_{eg}^4 [R_i(\omega_3, t_2, \omega_1) + R_{iii}(\omega_3, t_2, \omega_1)] + \mu_{eg}^2 \mu_{ef}^2 R_v(\omega_3, t_2, \omega_1) \right\} \tag{9}$$

We shall also display the following combination which shows absorptive peaks<sup>24,25</sup>.

$$S_A(\omega_3, t_2, \omega_1) \equiv -Im [S_I(\omega_3, t_2, -\omega_1) + S_{II}(\omega_3, t_2, \omega_1)] \tag{10}$$

When during the interval  $t_3$  the system has no memory about its state in  $t_1$  the third order response functions are factorized into products of the linear response functions  $K(t)$

$$R_i(t_3, t_2, t_1) = K(t_3)K(t_1)$$

$$R_{ii}(t_3, t_2, t_1) = K(t_3)K^*(t_1); \quad R_{ii}(\omega_3, t_2, \omega_1) = K(\omega_3)K^*(-\omega_1); \quad (11)$$

Neglecting the overtone contributions  $R_v$  and  $R_{vi}$  it follows that the  $S_A$  signal is given by the product of the linear lineshapes  $W_A$

$$\hbar S_A(\omega_3, \omega_1) = W_A(\omega_1)W_A(\omega_3). \quad (12)$$

#### IV. STOCHASTIC LIOUVILLE EQUATIONS FOR THE TWO-STATE-JUMP MODEL

We first consider the TSJ model<sup>7,17,18</sup> by neglecting the spectral diffusion (setting  $\Delta_2, \Delta_3, \Omega_2, \Omega_3 = 0$ ). The total density matrix  $\rho$  has 18 components  $|\nu\nu's\rangle\rangle$  given by the direct product of 9 Liouville space states  $|\nu\nu'\rangle\rangle$  and the two spin states,  $s = u, d$ . The SLE<sup>11,26</sup> then reads

$$\frac{d\rho}{dt} = \hat{\mathcal{L}}\rho(t). \quad (13)$$

The Liouville operator  $\hat{\mathcal{L}}$  is diagonal in the vibrational Liouville space variables, and is thus given by nine  $2 \times 2$  diagonal blocks in spin space,

$$\left[ \hat{\mathcal{L}} \right]_{\nu\nu's, \nu_1\nu_1's'} = \delta_{\nu\nu_1} \delta_{\nu'\nu_1'} \left[ \hat{\mathcal{L}}_S \right]_{s,s'} + \delta_{\nu\nu_1} \delta_{\nu'\nu_1'} \delta_{ss'} \left[ \hat{\mathcal{L}}_{SV} \right]_{\nu\nu's, \nu\nu's} \quad (14)$$

where  $\hat{\mathcal{L}}_S$  describes the two state jump kinetics and  $\hat{\mathcal{L}}_{SV}$  represents the coherent vibrational evolution that depends parametrically on the spin state.

Chemical exchange is described by the rate matrix  $\hat{\mathcal{L}}_S$  for the spin:

$$\left[ \hat{\mathcal{L}}_S \right] = \begin{pmatrix} -k_d & k_u \\ k_d & -k_u \end{pmatrix} \quad (15)$$

The up (down) jump rates  $k_u, (k_d)$  are connected by the detailed-balance relation  $k_u/k_d = \exp \beta(\epsilon_d - \epsilon_u)$ , where  $\epsilon_d - \epsilon_u$  is the energy difference between the  $u$  and  $d$  states.

The equilibrium density matrix is

$$|\rho(0)\rangle\rangle = |gg\rangle\rangle |\rho(0)\rangle_s; \quad |\rho(0)\rangle_s = \frac{1}{k_u + k_d} \begin{pmatrix} k_u \\ k_d \end{pmatrix}. \quad (16)$$

We next turn to the vibrational part  $\hat{\mathcal{L}}_{SV} \equiv -(i/\hbar)[H_{SV}, \dots]$ . For the  $|gg\rangle\rangle, |ee\rangle\rangle, |ff\rangle\rangle$  blocks  $\left[ \hat{\mathcal{L}}_{SV} \right]_{gg,gg} = \left[ \hat{\mathcal{L}}_{SV} \right]_{ee,ee} = \left[ \hat{\mathcal{L}}_{SV} \right]_{ff,ff} = 0$ . The other blocks of  $\mathcal{L}_{SV}$  are:

$$\left[ \hat{\mathcal{L}}_{SV} \right]_{eg,eg} = \begin{pmatrix} -i(\Omega_0 + \Omega_1) & 0 \\ 0 & -i(\Omega_0 - \Omega_1) \end{pmatrix}$$

$$\begin{aligned} \left[ \hat{\mathcal{L}}_{SV} \right]_{fe,fe} &= \begin{pmatrix} -i(\Omega_0 + \Delta_0) - i(\Omega_1 + \Delta_1) & 0 \\ 0 & -i(\Omega_0 + \Delta_0) + i(\Omega_1 + \Delta_1) \end{pmatrix} \\ \left[ \hat{\mathcal{L}}_V \right]_{fg,fg} &= \begin{pmatrix} -i(2\Omega_0 + \Delta_0) - i(2\Omega_1 + \Delta_1) & 0 \\ 0 & -i(2\Omega_0 + \Delta_0) + i(2\Omega_1 + \Delta_1) \end{pmatrix} \end{aligned}$$

The remaining blocks are obtained by taking complex conjugates  $\left[ \hat{\mathcal{L}}_{SV} \right]_{\nu\nu',\nu\nu'} = \left[ \hat{\mathcal{L}}_{SV} \right]_{\nu'\nu,\nu'\nu'}^*$ .

These matrices may be represented in a compact form by defining the energy  $\hbar\epsilon_0$  and splitting  $\hbar\epsilon_1$  parameters  $\epsilon_0^{(g)} = 0$ ,  $\epsilon_0^{(e)} = \Omega_0$ ,  $\epsilon_0^{(f)} = 2\Omega_0 + \Delta_0$ ,  $\epsilon_1^{(g)} = 0$ ,  $\epsilon_1^{(e)} = \Omega_1$ ,  $\epsilon_1^{(f)} = 2\Omega_1 + \Delta_1$ . We then have

$$\left[ \hat{\mathcal{L}}_{SV} \right]_{\nu\nu',\nu_1\nu_1'} = \delta_{\nu\nu_1} \delta_{\nu'\nu_1'} \begin{pmatrix} -i(\epsilon_0^{(\nu)} - \epsilon_0^{(\nu')}) - i(\epsilon_1^{(\nu)} - \epsilon_1^{(\nu')}) & 0 \\ 0 & -i(\epsilon_0^{(\nu)} - \epsilon_0^{(\nu')}) + i(\epsilon_1^{(\nu)} - \epsilon_1^{(\nu')}) \end{pmatrix} \quad (17)$$

The Green's function solution of Eq. (13) is given by  $2 \times 2$  blocks for each vibrational state  $|\nu\nu'\rangle\rangle$  of the density matrix

$$\begin{aligned} \left[ \mathcal{G} \right]_{\nu\nu',\nu_1\nu_1'}(t) &\equiv \left[ \exp(\hat{\mathcal{L}}t) \right]_{\nu\nu',\nu_1\nu_1'} = \delta_{\nu\nu_1} \delta_{\nu'\nu_1'} \\ &\times \left\{ \left( \frac{\eta_2}{\eta_2 - \eta_1} \hat{1} - \frac{1}{\eta_2 - \eta_1} \hat{\mathcal{L}}_{\nu\nu',\nu\nu'} \right) \exp(\eta_1 t) + \left( \frac{\eta_1}{\eta_1 - \eta_2} \hat{1} - \frac{1}{\eta_1 - \eta_2} \hat{\mathcal{L}}_{\nu\nu',\nu\nu'} \right) \exp(\eta_2 t) \right\} \end{aligned} \quad (18)$$

where  $\eta_j$  are the eigenvalues of each block of  $\hat{\mathcal{L}}$

$$\eta_1 = -\frac{k_d + k_u}{2} - i(\epsilon_0^{(\nu)} - \epsilon_0^{(\nu')}) + \sqrt{\frac{(k_d + k_u)^2}{4} - (\epsilon_1^{(\nu)} - \epsilon_1^{(\nu')})^2 + i(\epsilon_1^{(\nu)} - \epsilon_1^{(\nu')})(k_d - k_u)}$$

$$\eta_2 = -\frac{k_d + k_u}{2} - i(\epsilon_0^{(\nu)} - \epsilon_0^{(\nu')}) - \sqrt{\frac{(k_d + k_u)^2}{4} - (\epsilon_1^{(\nu)} - \epsilon_1^{(\nu')})^2 + i(\epsilon_1^{(\nu)} - \epsilon_1^{(\nu')})(k_d - k_u)}$$

For the  $gg, ee$  and  $ff$  space  $\hat{\mathcal{L}}_{SV} = 0$ , and Eq.(18) reads

$$\mathcal{G}_{ee,ee}(t) = \mathcal{G}_{gg,gg}(t) = \mathcal{G}_{ff,ff}(t) \equiv \exp(\hat{\mathcal{L}}st) = \hat{1} + \frac{1 - \exp[-(k_d + k_u)t]}{k_d + k_u} \begin{pmatrix} -k_d & k_u \\ k_d & -k_u \end{pmatrix} \quad (19)$$

The linear response is given in Appendix A. Closed form expressions for the various pathways are given in the Appendix B. Below we discuss the 2D signals for limiting cases.

In the slow bath limit  $\Omega_1 \gg k$  (In Figs 2-6  $k \equiv k_d = k_u$ ) no spin jumps occur during the  $t_1$ , and  $t_3$  intervals. In Fig 2a we display the 2D lineshapes  $S_A$  (Eq.(10)). In all figures

we give frequencies with respect to  $\Omega_0$  (i.e. we set  $\Omega_0 = 0$ ) and normalize the signal to have maximum absolute value of 1. For  $kt \ll 1$  no spin jumps occur during the  $t_2$  interval and we only see 4 peaks (Fig 2a) two diagonal at  $\omega_1 = \omega_3 = \Omega_0 \pm \Omega_1$  and two overtone at  $(\omega_1, \omega_3) = (\Omega_0 + \Omega_1, \Omega_0 + \Delta_0 + \Omega_1 + \Delta_1)$  and  $(\Omega_0 - \Omega_1, \Omega_0 + \Delta_0 - \Omega_1 - \Delta_1)$ . In the opposite  $kt_2 \gg 1$  limit we see 8 peaks (Fig 2b). In addition to the previous four peaks cross peaks appears at  $(\omega_1, \omega_3) = (\Omega_0 + \Delta_0, \Omega_0 - \Delta_0), (\Omega_0 - \Delta_0, \Omega_0 + \Delta_0), (\Omega_0 - \Omega_1, \Omega_0 + \Delta_0 + \Omega_1 + \Delta_0), (\Omega_0 + \Omega_1, \Omega_0 - \Omega_1 + \Delta_0 - \Delta_1)$  due to the spin jumps. Diagrams *i*, *ii*, *iii*, and *iv* describe the *g* to *e* peaks at  $\omega_1, \omega_3 \sim \Omega$ . Diagrams *v* and *vi* show the *e* to *f* peaks at  $\omega_1 \sim \Omega + \Delta$ .

Note that the relation (Eq.(B5)), similar to Eq.(12) is valid for *individual* peaks in the short time regime since peak shapes are not connected with any inhomogeneity which carries memory, however Eq.(12) does not apply for the whole 2D shape, since the memory of spin state erases the cross peaks. In contrast, for long  $t_2$  (Fig 2b) this memory is lost and Eq.(12) applies (excluding the overtone contributions).

In Fig 2c we plot  $S_A$  (Eq.10) in the fast  $k_u, k_d \gg \Omega_1$  limit. We see a fundamental peak at  $\omega_1 = \omega_3 = \Omega_0$  and an overtone peak at  $\omega_1 = \Omega_1, \omega_3 = \Omega_0 + \Delta_0$ . Linear response in fast regime shows one peak (fluctuational narrowing<sup>17</sup>). Any memory of  $t_1$  interval is lost in the  $t_3$  interval and the factorization (Eq.11) is valid resulting in Eq. 12 which is observed in Fig 2c.

## V. TWO-STATE-JUMP WITH SPECTRAL DIFFUSION

Spectral diffusion is described by a dimensionless overdamped Brownian oscillator coordinate  $Q$  (Eq.(1)) whose variance 1 and its dynamics is given by the Fokker-Planck operator<sup>27</sup>

$$\mathcal{L}_Q = \Lambda \frac{\partial}{\partial Q} \left( Q + \frac{\partial}{\partial Q} \right) \quad (20)$$

where  $\Lambda$  is the relaxation rate. For fast fluctuations  $\Omega_2/\Lambda \ll 1$ , spectral diffusion may be accounted for by simply adding dephasing rates  $\Omega_2^2/\Lambda$  to the lineshapes. The complete solution of the Fokker-Planck equation is required for arbitrary fluctuation timescales.

We define  $\epsilon_2^{(g)} = 0$ ,  $\epsilon_2^{(e)} = \Omega_2$ ,  $\epsilon_2^{(f)} = 2\Omega_2 + \Delta_2$ , and  $\epsilon_3^{(g)} = 0$ ,  $\epsilon_3^{(e)} = \Omega_3$ ,  $\epsilon_3^{(f)} = 2\Omega_3 + \Delta_3$ . The coupling of  $Q$  to the vibration is given by the Liouville operator  $\hat{\mathcal{L}}_{QV}$

$$\begin{aligned} \left[ \hat{\mathcal{L}}_{QV} \right]_{\nu\nu's, \nu_1\nu_1's_1} &= -i \left( \epsilon_2^{(\nu)} - \epsilon_2^{(\nu')} \right) Q \delta_{\nu\nu_1} \delta_{\nu'\nu_1'} \delta_{ss_1} \\ \left[ \hat{\mathcal{L}}_{SQV} \right]_{\nu\nu's, \nu_1\nu_1's_1} &- i \left( \epsilon_3^{(\nu)} - \epsilon_3^{(\nu')} \right) Q \delta_{\nu\nu_1} \delta_{\nu'\nu_1'} [\sigma_z]_{ss_1} \end{aligned} \quad (21)$$



The complete Liouville superoperator describing both TSJ and BO fluctuations is finally given by:

$$\hat{\mathcal{L}}_{tot} = \hat{\mathcal{L}}_S + \hat{\mathcal{L}}_{SV} + \hat{\mathcal{L}}_{QV} + \hat{\mathcal{L}}_{SQV} + \mathcal{L}_Q \quad (22)$$

where  $\hat{\mathcal{L}}_S$  is given by Eq. (15),  $\hat{\mathcal{L}}_{SV}$  by Eqs.(17),  $\hat{\mathcal{L}}_{QV}, \hat{\mathcal{L}}_{SQV}$  by Eqs.(21), and  $\mathcal{L}_Q$  by Eq.(20).

The response function for the spectral diffusion model alone<sup>28</sup> (neglecting the spin, setting  $\Omega_1 = 0, \Delta_1 = 0$ ) can be calculated using the second order cumulant expansion<sup>23</sup> and is given in Appendix C.

We next turn to the third order response (Eq.(6)). The equilibrium distribution is

$$|\rho(0)\rangle_{QS} = |\rho(0)\rangle_S |0\rangle_Q \quad (23)$$

where  $|\rho(0)\rangle_S$  is given by Eq.(16) and  $|0\rangle_Q$  by Eq. (D1) and the final averaging should run over all degrees of freedom.

$$\langle I |_{QS} = \langle I |_S \langle 0 |_Q$$

The Green's function matrix elements  $\mathcal{G}_{fe,fe}(t_3)$  are now matrices in the joint spin and BO space

$$\mathcal{G}_{\nu\nu',\nu_1\nu'_1}(\omega) = - \left( \left[ i\omega + \hat{\mathcal{L}}_{tot} \right]_{\nu\nu',\nu_1\nu'_1} \right)^{-1}. \quad (24)$$

$\mathcal{G}(\omega_1)$ ,  $\mathcal{G}(\omega_3)$  are calculated in Appendix E by expanding them in the Fokker-Planck eigenmodes<sup>15,16,27,29</sup>.

During  $t_2$  the evolution is in the  $ee, gg, ff$  space where  $\hat{\mathcal{L}}_{QS} = 0$  and the Green's function may be factorized as

$$\mathcal{G}_{ee,ee}(t_2) = \mathcal{G}_{gg,gg}(t_2) = \exp \left( \hat{\mathcal{L}}_S t_2 \right) \exp \left( \mathcal{L}_Q t_2 \right) \quad (25)$$

where the first factor is given by Eq.(19) and the second term is the propagator of Fokker-Planck equation<sup>27</sup> expanded in its eigenmodes (Eq.(D1))

$$[\exp(\mathcal{L}_Q t)]_{\alpha\beta} = \delta_{\alpha\beta} \exp(-\alpha \Lambda t) \quad (26)$$

For slow chemical exchange compared to the spectral diffusion ( $k_u, k_d \ll \sigma, \Lambda$ ) the TSJ peaks are well resolved and their lineshapes are determined by the spectral diffusion. Chemical exchange occurs on a much longer timescale and affects the cross peaks.

We start by setting  $\Omega_3, \Delta_3 = 0$  and examine fast and the slow spectral diffusion. The fast (motional narrowing) limit ( $\Lambda \gg \Omega_2$ ) gives a Lorentzian absorption lineshape. Since the

bath has no memory, peak shapes are less sensitive to  $t_2$  and cross peaks due to chemical exchange only appear as  $t_2$  is increased. Effects of fast fluctuations may be accounted for by adding dephasing rates  $\Omega_2^2/\Lambda$ . 2D-lineshapes  $S_A$  (Eq. (10) shown in Fig 3 are similar to the TSJ model (Fig 2), both are given by a product of Lorentzian lineshapes (in  $\omega_1, \omega_3$ ). The important difference is that when accounting for fast spectral diffusion, the linewidth is determined by both exchange and dephasing rates  $(k_d + \Omega_2^2/\Lambda)^{-1}$ , i.e. it is different from the cross-peak timescale. In contrast the linewidth of TSJ model must be equal to exchange rate  $k$  obtained by analysis of the cross-peaks growth.

$S_A$  in the static  $\Lambda \ll \Omega_2$  limit (Fig 4) shows Gaussian linear lineshapes. Static disorder is eliminated in the photon echo  $\mathbf{k}_I$  experiment. 2D peaks are elliptic with different "diagonal" and "off-diagonal" linewidths (Fig 4a)<sup>30</sup>. The intermediate regime may be observed at  $\Lambda^{-1} < t_2 < k^{-1}$  when the bath loses memory (Fig 4b) and the 2D peaks become symmetric. For long times  $k_d t_2 \gg 1$  we see cross peaks induced by chemical exchange. Note the circular contours of Fig 4c, compared to the star-like contours for fast fluctuations (Fig 3). These may be understood by noting that the product of two Gaussians (which represent the linear lineshape for the slow case) is rotationally invariant, unlike the Lorentzian lineshapes in the fast limit.

Fig 5 shows the  $\mathbf{k}_I$  and  $\mathbf{k}_{II}$  signals (Eqs. (8), and (9)) . The  $\mathbf{k}_I$  contribution dominates at short times, and shows effective rephasing (photon echo) and the final 2DIR is similar to this dominating  $\mathbf{k}_I$  contribution (See Fig 4a.). The bath loses memory of its initial state in the third interval. For longer  $t_2 \gg \Lambda^{-1}$  (right panels), the  $\mathbf{k}_I$  and  $\mathbf{k}_{II}$  contributions become comparable and  $S_A$  becomes symmetric (see Fig 4).

We next explore some more general cases. First we take  $\Delta_2 \neq 0$ . The overtone peaks may then show different widths along  $\omega_3$  and  $\omega_1$ . (overtone photon echoes are expected at  $\Omega_2 t_1 = (\Omega_2 + \Delta_2) t_3$  ) Note that we have a slow bath ( $\Lambda < \Omega_2$ ) for the *eg* and a fast bath for the *ef* transition ( $\Lambda > \Omega_2 + \Delta_2$ ). These lineshapes are shown in Fig. 6.

The inclusion of  $\Omega_3$  does not require additional numerical effort. This parameter allows the *u* and *d* peaks have a different width due the spectral diffusion.

To demonstrate these effects and relate them to recent experiments<sup>1</sup> we have simulated the spectral diffusion using a single overdamped Brownian coordinate allowing a different width for *u* and *d* peaks. We used the splitting  $2\Delta_0 = 34\text{cm}^{-1}$  (i.e.  $\sim 1.01\text{ps}^{-1}$ ) and the exchange rates  $k_u = 0.1\text{ps}^{-1}$   $k_d = 0.125\text{ps}^{-1}$  which were determined in<sup>1</sup> from the cross peaks

growth. Three regimes similar to those of Fig 4 were observed<sup>1</sup> suggesting that the bath is not fast. The intermediate regime, where the memory of the BO coordinate is lost (circular lineshape) but the cross peaks are still weak, was found on the 2ps timescale. We thus assumed for the relaxation rate  $\Lambda \sim 0.4ps^{-1}$ . Knowing  $\Lambda$ ,  $\Omega_1$  and  $\Omega_3$  are connected to the peak linewidth in linear spectra and can be estimated using the Pade approximant of a 2-level system<sup>23,31</sup>. We have simulated the absorption spectra in Fig 7 and found lineshapes similar to experiment for  $\Omega_2 = 0.33ps^{-1}$ ,  $\Omega_3 = -0.07ps^{-1}$ . This completely determines the model for 2D IR spectroscopy (neglecting dynamics in the overtone), we have no additional free parameter. In Fig 18 we show that the predicted 2DIR lineshapes of the same model are in qualitative agreement with experiment. We see all three regimes, rephasing elliptic shapes, the relaxed Brownian oscillator with circular shape and chemical exchange cross-peaks at the proper timescales. The peaks have also the correct relative intensity the lower frequency peak is weaker but broader.

In conclusion, we have demonstrated that the SLE may be used to model chemical exchange in 2DIR spectroscopy. Spectral diffusion can no longer be accounted for in terms of dephasing rates, when its timescale may be observed in experiment and its proper description must be combined with the two state jump which describe chemical exchange. The high temperature overdamped Brownian oscillator model for spectral diffusion with arbitrary fluctuation timescale reproduces the most significant features of recent experiments<sup>1</sup>.

In contrast with calculations based on cumulant expansions at finite temperatures<sup>16,23,32</sup> our high temperature bath does not respond to the state of system, and its evolution in the ground and excited state is same. This may limit the applicability of SLE model when signatures of the vibrational Stokes shift are observed in 2DIR signals, however it simplifies the calculations. The lack of phase factors during the  $t_2$  interval reduces the dynamics to classical level and allows large scale MD simulations of environmental dynamics.

### Acknowledgments

The support of NSF (Grant No CHE-0446555) and NIH (2RO1GM59230-05) is gratefully acknowledged. F. Š. is also supported by the Ministry of Education, Youth and Sports of the Czech Republic (project MSM 0021620835).

## APPENDIX A: THE ABSORPTION LINESHAPE

The linear response function is given by<sup>23</sup>

$$S^{(1)}(t_1) = \theta(t_1) \frac{i}{\hbar} \langle \langle I | \mu^{(-)} \mathcal{G}(t_1) \mu^{(-)} | \rho(0) \rangle \rangle_{\mathcal{H}}$$

We define the contribution

$$K(t_1) = \langle I | \mathcal{G}_{eg,eg}(t_1) | \rho(0) \rangle_{QS}.$$

This response function is connected to absorption lineshape

$$W(\omega_1) = \mu_{eg}^2 \hbar^{-1} \text{Re} \int_0^\infty \exp(i\omega_1 t_1) K(t_1) dt_1 \quad (\text{A1})$$

For the TSJ model ( $\Omega_{2,3} = 0$ ) the result of Kubo<sup>17</sup> is recovered:

$$W(\omega) = \frac{1}{(k_d + k_u)} \times \frac{4k_d k_u \Omega_1^2}{(\omega - \Omega_0 - \Omega_1)^2 + [(\omega - \Omega_0)(k_d + k_u) + \Omega_1(k_d - k_u)]^2}$$

For the spectral diffusion model we set  $\Omega_1 = 0$  and the linear response function is given by the second order cumulant expression (see Eq. (C6)).

$$K(t_1) = \exp(-g_{ee}(t_1))$$

## APPENDIX B: RESPONSE FUNCTIONS FOR TWO-STATE-JUMP SPIN DYNAMICS

In the frequency domain the Green's function (Eq. 18) matrix elements are:

$$\begin{aligned} \mathcal{G}_{\nu\nu',\nu_1\nu'_1}(\omega) &= - \left[ (i\omega + \hat{\mathcal{L}})^{-1} \right]_{\nu\nu',\nu_1\nu'_1} = \\ &= \frac{-\delta_{\nu\nu_1} \delta_{\nu'\nu'_1}}{(\omega - \epsilon_0^{(\nu)} + \epsilon_0^{(\nu')})^2 - (\epsilon_1^{(\nu)} - \epsilon_1^{(\nu')})^2 + i(\omega - \epsilon_0^{(\nu)} + \epsilon_0^{(\nu')})(k_d + k_u) + i(\epsilon_1^{(\nu)} - \epsilon_1^{(\nu')})(k_d - k_u)} \\ &\quad \times \begin{pmatrix} k_u - i(\omega - \epsilon_0^{(\nu)} + \epsilon_0^{(\nu')} + \epsilon_1^{(\nu)} - \epsilon_1^{(\nu')}) & k_u \\ k_d & k_d - i(\omega - \epsilon_0^{(\nu)} + \epsilon_0^{(\nu')} - \epsilon_1^{(\nu)} + \epsilon_1^{(\nu')}) \end{pmatrix} \quad (\text{B1}) \end{aligned}$$

$R_i$  and  $R_{ii}$  (Eq.6) are given by:

$$R_\alpha(\omega_3, t_2, \omega_1) = \frac{1}{(\omega_1 \mp \Omega_0)^2 - \Omega_1^2 + i(\omega_1 \mp \Omega_0)(k_d + k_u) \pm i\Omega_1(k_d - k_u)}$$

$$\begin{aligned}
& \times \frac{1}{(\omega_3 - \Omega_0)^2 - \Omega_1^2 + i(\omega_3 - \Omega_0)(k_d + k_u) + i\Omega_1(k_d - k_u)} \frac{1}{k_u + k_d} \\
& \times \left\{ (k_u + k_d)^3 - [(\omega_3 - \Omega_0)(\omega_1 \mp \Omega_0) \pm \Omega_1^2] (k_u + k_d) + [(\omega_1 \mp \Omega_0)\Omega_1 \pm (\omega_3 - \Omega_0)\Omega_1] (k_d - k_u) \right. \\
& \quad - i [(\omega_3 - \Omega_0 + \omega_1 \mp \Omega_0)(k_u + k_d)^2 - (\Omega_1 \pm \Omega_1)(k_d^2 - k_u^2)] \\
& \quad \left. \pm 4\Omega_1^2 k_u k_d \frac{1 - \exp[-(k_d + k_u)t_2]}{k_d + k_u} \right\}
\end{aligned}$$

where the upper (lower) sign is for  $R_i$  ( $R_{ii}$ ). Since the evolution in the excited  $|ee\rangle$  and in the ground  $|gg\rangle$  state is the same for stochastic jumps (where the bath is not affected by the system) we have

$$R_{iii}(\omega_3, t_2, \omega_1) = R_i(\omega_3, t_2, \omega_1); \quad R_{iv}(\omega_3, t_2, \omega_1) = R_{ii}(\omega_3, t_2, \omega_1) \quad (\text{B2})$$

We further have for  $R_v$  and  $R_{vi}$ :

$$\begin{aligned}
R_\alpha(\omega_3, t_2, \omega_1) &= -\frac{1}{(\omega_1 \mp \Omega_0)^2 - \Omega_1^2 + i(\omega_1 \mp \Omega_0)(k_d + k_u) \pm i\Omega_1(k_d - k_u)} \\
& \times \frac{1}{(\omega_3 - \Omega_0 - \Delta_0)^2 - (\Omega_1 + \Delta_1)^2 + i(\omega_3 - \Omega_1 - \Delta_1)(k_d + k_u) + i(\Omega_1 + \Delta_1)(k_d - k_u)} \\
& \times \frac{1}{k_u + k_d} \left\{ (k_u + k_d)^3 - [(\omega_3 - \Omega_0 - \Delta_0)(\omega_1 \mp \Omega_0) \pm (\Omega_1 + \Delta_1)\Omega_1] (k_u + k_d) \right. \\
& \quad + [(\omega_1 \mp \Omega_1)(\Omega_1 + \Delta_1) \pm (\omega_3 - \Omega_0 - \Delta_0)\Omega_1] (k_d - k_u) \\
& \quad - i [(\omega_3 - \Omega_0 - \Delta_0 + \omega_1 \mp \Omega_0)(k_u + k_d)^2 - (\Omega_1 + \Delta_1 \pm \Omega_1)(k_d^2 - k_u^2)] \\
& \quad \left. \pm 4(\Omega_1(\Omega_1 + \Delta_1)k_u k_d \frac{1 - \exp[-(k_d + k_u)t_2]}{k_d + k_u}) \right\}
\end{aligned}$$

where the upper (lower) sign is for  $R_v$  ( $R_{vi}$ ).

### 1. High temperature spin dynamics

In the high temperature limit we set  $k_u = k_d \equiv k$ . We first analyze the  $R_i, R_{ii}$  contributions. Here

$$\mathcal{G}_{eg,eg}(t) = e^{-(k+i\Omega_0)t} \begin{pmatrix} \cosh(\eta t) - \frac{i\Omega_1}{\eta} \sinh(\eta t) & \frac{k}{\eta} \sinh(\eta t) \\ \frac{k}{\eta} \sinh(\eta t) & \cosh(\eta t) + \frac{i\Omega_1}{\eta} \sinh(\eta t) \end{pmatrix} \quad (\text{B3})$$

and

$$\mathcal{G}_{ge,ge}(t) = \mathcal{G}_{eg,eg}^*(t)$$

where  $\eta = \sqrt{k^2 - \Omega_1^2}$ . When  $\Omega_1 > k$  we use analytic continuation (e.g.  $\cosh(ix) = \cos x$  and  $\sinh(ix) = i \sin x$ ) and after some algebra we get for  $\alpha = i, ii$ <sup>19</sup>

$$R_\alpha(t_3, t_2, t_1) = \frac{e^{-k(t_1+t_3)} e^{-i\Omega(t_3 \pm t_1)}}{2} \times \left[ \left(1 + \frac{k^2}{\eta^2}\right) \cosh[\eta(t_1 + t_3)] + \left(1 - \frac{k^2}{\eta^2}\right) \cosh[\eta(t_1 - t_3)] + \frac{2k}{\eta} \sinh[\eta(t_1 + t_3)] \right] \mp e^{-k(t_1+2t_2+t_3)} e^{-i\Omega(t_3 \pm t_1)} \frac{\omega_0^2}{2\eta^2} [\cosh[\eta(t_1 + t_3)] - \cosh[\eta(t_1 - t_3)]] \quad (\text{B4})$$

where the upper (lower) sign stands for  $R_i$  ( $R_{ii}$ ). Eq. (7 then gives

$$R_\alpha(\omega_3, t_2, \omega_1) = \frac{1}{(\omega_1 \mp \Omega_0)^2 - \Omega_1^2 + 2i(\omega_1 \mp \Omega_0)k} \times \frac{1}{(\omega_3 - \Omega_0)^2 - \Omega_1^2 + 2i(\omega_3 - \Omega_0)k} \left\{ 4k^2 - (\omega_3 - \Omega_0)(\omega_1 \mp \Omega_0) \mp \Omega_1^2 - 2i(\omega_3 - \Omega_0 + \omega_1 \mp \Omega_0)k \pm \Omega_1^2 [1 - \exp(-2kt_2)] \right\}$$

We further have  $R_{iii} = R_i$ ,  $R_{iv} = R_{ii}$ . For  $\alpha = v, vi$  we get

$$R_\alpha(\omega_3, t_2, \omega_1) = \frac{1}{(\omega_1 \mp \Omega_0)^2 - \Omega_1^2 + 2i(\omega_1 \mp \Omega_0)k} \times \frac{1}{(\omega_3 - \Omega_0 - \Delta_0)^2 - (\Omega_1 + \Delta_1)^2 + 2i(\omega_3 - \Omega_1 - \Delta_1)k} \times \left\{ 4k^2 - [(\omega_3 - \Omega_0 - \Delta_0)(\omega_1 \mp \Omega_0) \pm (\Omega_1 + \Delta_1)\Omega_1] - 2i[(\omega_3 - \Omega_0 - \Delta_0 + \omega_1 \mp \Omega_0)k] \pm \Omega_1(\Omega_1 + \Delta_1)(1 - \exp[-2kt_2]) \right\}$$

where the upper (lower) sign corresponds to  $R_v$  ( $R_{vi}$ ).

## 2. Slow spin dynamics

When assume  $\Omega_1 \gg k_u, k_d$  no spin jumps occur during the  $t_1$ , and  $t_3$  intervals. Then

$$\mathcal{G}_{\nu\nu', \nu_1\nu_1'}(\omega) = \delta_{\nu\nu_1} \delta_{\nu'\nu_1'} \begin{pmatrix} k_d + i(\epsilon_0^{(\nu)} - \epsilon_0^{(\nu')} + \epsilon_1^{(\nu)} - \epsilon_1^{(\nu')} - \omega) & 0 \\ 0 & k_u + i(\epsilon_0^{(\nu)} - \epsilon_0^{(\nu')} - \epsilon_1^{(\nu)} + \epsilon_1^{(\nu')} - \omega) \end{pmatrix}^{-1}$$

The Green's function for  $t_2$  is still given by Eq. (19).

In the vicinity of the peaks (Fig 2a) at e.g.  $\omega_1 \approx \Omega_0 + \Omega_1$ ,  $\omega_3 \approx \Omega_0 - \Omega_1$  we have

$$R_i(\omega_3, 0, \omega_1) \propto \frac{1}{k_u - i(\omega_1 - \Omega_0 - \Omega_1)} \frac{1}{k_d - i(\omega_3 - \Omega_0 + \Omega_1)}$$

$$\begin{aligned}
&= \frac{k_d k_u - (\omega_1 - \Omega_0 - \Omega_1)(\omega_3 - \Omega_0 + \Omega_1) + i [k_d(\omega_1 - \Omega_0 - \Omega_1) + k_u(\omega_3 - \Omega_0 + \Omega_1)]}{(k_u^2 + (\omega_1 - \Omega_0 - \Omega_1)^2)(k_d^2 + (\omega_3 - \Omega_0 + \Omega_1)^2)} \\
&\quad R_{ii}(\omega_3, 0, \omega_1) \propto \frac{1}{k_u - i(\omega_1 + \Omega_0 + \Omega_1)} \frac{1}{k_d - i(\omega_3 - \Omega_0 + \Omega_1)} \\
&= \frac{k_d k_u - (\omega_1 + \Omega_0 + \Omega_1)(\omega_3 - \Omega_0 + \Omega_1) + i [k_d(\omega_1 + \Omega_0 + \Omega_1) + k_u(\omega_3 - \Omega_0 + \Omega_1)]}{(k_u^2 + (\omega_1 + \Omega_0 + \Omega_1)^2)(k_d^2 + (\omega_3 - \Omega_0 + \Omega_1)^2)}
\end{aligned}$$

In the absorptive signal (Eq.(10)) the dispersive parts (the second term in nominator) cancel out and the signal is given by simple lorentzian linear response peaks

$$S_A(\omega_3, 0, \omega_1) \propto \frac{4\mu_{eg}^4 k_d k_u}{\hbar^3 (k_u^2 + (\omega_1 - \Omega_0 - \Omega_1)^2)(k_d^2 + (\omega_3 - \Omega_0 + \Omega_1)^2)} = \hbar^{-1} W(\omega_1) W(\omega_3) \quad (\text{B5})$$

### 3. Fast spin fluctuations; motional narrowing

In the  $k_u, k_d \gg \Omega_1$  limit we get

$$\begin{aligned}
\mathcal{G}_{eg,eg}(\omega) &= \frac{-1}{(\omega - \Omega_0)^2 + i(\omega - \Omega_0)(k_d + k_u)} \begin{pmatrix} k_u - i(\omega - \Omega_0) & k_u \\ k_d & k_d - i(\omega - \Omega_0) \end{pmatrix} \\
\mathcal{G}_{ge,ge}(\omega) &= \mathcal{G}_{eg,eg}(-\omega)^*
\end{aligned}$$

The ine shapes is insensitive to  $t_2$  delay one can set

$$\mathcal{G}_{ee,ee}(t_2) = \mathcal{G}_{gg,gg}(t_2) = \frac{1}{k_u + k_d} \begin{pmatrix} k_u & k_u \\ k_d & k_d \end{pmatrix} = \frac{1}{k_u + k_d} \begin{pmatrix} k_u \\ k_d \end{pmatrix} \begin{pmatrix} 1 & 1 \end{pmatrix}$$

The response functions may now be factorized into products of the linear response functions (Eq. (11)).

## APPENDIX C: THE CUMULANT EXPANSION FOR THE SPECTRAL DIFFUSION MODEL

Neglecting spin dynamics by setting  $\Delta_1 = \Delta_3 = 0, \Omega_1 = \Omega_3 = 0$ , the response functions may be calculated by the second order cumulant expansion<sup>23,33</sup> which represents stochastic Gaussian fluctuations.

The response function may be expressed in terms of the following four-point correlation functions<sup>34</sup>:

$$\begin{aligned}
F_1(\tau_4, \tau_3, \tau_2, \tau_1) &\equiv \langle B(\tau_4) B^\dagger(\tau_3) B(\tau_2) B^\dagger(\tau_1) \rangle \\
F_2(\tau_4, \tau_3, \tau_2, \tau_1) &\equiv \langle B(\tau_4) B(\tau_3) B^\dagger(\tau_2) B^\dagger(\tau_1) \rangle / 2.
\end{aligned} \quad (\text{C1})$$

We then have<sup>34,35,36</sup>:

$$\begin{aligned}
R_i(t_3, t_2, t_1) &= F_1(t_1, t_1 + t_2, t_1 + t_2 + t_3, 0) \\
R_{ii}(t_3, t_2, t_1) &= F_1(0, t_1 + t_2, t_1 + t_2 + t_3, t_1) \\
R_{iii}(t_3, t_2, t_1) &= F_1(t_1 + t_2 + t_3, t_1 + t_2, t_1, 0) \\
R_{iv}(t_3, t_2, t_1) &= F_1(0, t_1, t_1 + t_2 + t_3, t_1 + t_2) \\
R_v(t_3, t_2, t_1) &= F_2(t_1, t_1 + t_2 + t_3, t_1 + t_2, 0) \\
R_{vi}(t_3, t_2, t_1) &= F_2(0, t_1 + t_2 + t_3, t_1 + t_2, t_1)
\end{aligned} \tag{C2}$$

Here:

$$F_1(\tau_4, \tau_3, \tau_2, \tau_1) = \exp[i(-\Omega_0\tau_4 + \Omega_0\tau_3 - \Omega_0\tau_2 + \Omega_0\tau_1) - f_1(\tau_4, \tau_3, \tau_2, \tau_1)] \tag{C3}$$

with:

$$\begin{aligned}
f_1(\tau_1, \tau_2, \tau_3, \tau_4) &= g_{ee}(t_{21}) + g_{ee}(t_{43}) + g_{ee}(t_{32}) + g_{ee}(t_{41}) - \\
&\quad - g_{ee}(t_{31}) - g_{ee}(t_{42}).
\end{aligned}$$

where  $t_{ij} \equiv \tau_i - \tau_j$  and

$$F_2(\tau_4, \tau_3, \tau_2, \tau_1) = \exp[i(-\Omega_0\tau_4 - (\Omega_0 + \Delta_0)\tau_3 + (\Omega_0 + \Delta_0)\tau_2 + \Omega_0\tau_1) - f_2(\tau_4, \tau_3, \tau_2, \tau_1)] \tag{C4}$$

with

$$\begin{aligned}
f_2(\tau_1, \tau_2, \tau_3, \tau_4) &= g_{ee}(t_{21}) + g_{ff}(t_{32}) + g_{ee}(t_{43}) - g_{ef}(t_{21}) - \\
&\quad - g_{ef}(t_{32}) + g_{ef}(t_{31}) + g_{ee}(t_{32}) + g_{ee}(t_{41}) - \\
&\quad - g_{ee}(t_{31}) - g_{ee}(t_{42}) - g_{fe}(t_{32}) - g_{fe}(t_{43}) + g_{fe}(t_{42}).
\end{aligned} \tag{C5}$$

$g_{ab}$  are the line broadening functions<sup>23,34</sup>

$$\begin{aligned}
g_{ee}(t) &= \Omega_2^2 [\exp(-\Lambda t) + \Lambda t - 1] \\
g_{ef}(t) &= (\Omega_2 + \Delta_2)\Omega_2 [\exp(-\Lambda t) + \Lambda t - 1] \\
g_{ff}(t) &= (\Omega_2 + \Delta_2)^2 [\exp(-\Lambda t) + \Lambda t - 1]
\end{aligned} \tag{C6}$$

Note that  $R_i = R_{iii}$ , and  $R_{ii} = R_{iv}$  as expected for stochastic models of frequency fluctuations .



## APPENDIX D: SPECTRUM OF THE FOKKER-PLANCK EQUATION

The eigenvectors of the Fokker-Planck operator Eq. (20) with eigenvalue  $-\alpha\Lambda$  are given by<sup>27</sup>

$$|\alpha\rangle_Q = \frac{\exp[-(Q^2/2)]}{2^n \sqrt{2\pi n!}} H_\alpha\left(\frac{Q}{\sqrt{2}}\right); \quad \alpha = 0, 1, 2, \dots \quad (\text{D1})$$

where  $H_\alpha$  is the Hermite polynomial

$$H_\alpha(x) = (-1)^n e^{x^2} \frac{d^\alpha}{dx^\alpha} e^{-x^2}$$

The matrix representation of bath densities and evolution matrices refer to to the basis  $\{|\alpha\rangle_Q\}$ . The matrix elements of  $\mathcal{L}_Q$  are

$$(\mathcal{L}_Q)_{\beta,\alpha} = -\alpha\Lambda\delta_{\alpha,\beta} \quad (\text{D2})$$

We use the recurrence relation:

$$QH_\alpha(Q) = \frac{H_{\alpha+1}(Q)}{2} + nH_{\alpha-1}(Q) \quad (\text{D3})$$

The  $Q$  coordinate is then represented by the tridiagonal matrix (Eq. (D4)).

$$[Q]_{\beta\alpha} = \beta\sqrt{2}\delta_{\beta,\alpha+1} + \frac{1}{\sqrt{2}}\delta_{\beta,\alpha-1} \quad (\text{D4})$$

## APPENDIX E: MATRIX CONTINUED-FRACTION SOLUTION OF THE FOKKER-PLANCK EQUATION

The complete Liouville superoperator is a  $18 \times 18$  matrix in the joint vibrational and spin space.

The  $Q$  variable is tridiagonal in the Fokker-Planck eigenbasis and the complete Liouvillean may be thus arranged in the tridiagonal block structure in the Brownian coordinate variable

$$i\omega + \hat{\mathcal{L}} = \begin{pmatrix} \mathcal{Q}_0 & \mathcal{Q}_0^+ & 0 & 0 & \dots & \dots \\ \mathcal{Q}_1^- & \mathcal{Q}_1 & \mathcal{Q}_1^+ & 0 & \dots & \dots \\ \dots & \dots & \dots & \dots & \dots & \dots \\ 0 & \dots & \mathcal{Q}_n^- & \mathcal{Q}_n & \mathcal{Q}_n^+ & \dots \\ \dots & \dots & \dots & \dots & \dots & \dots \end{pmatrix} \quad (\text{E1})$$

For Eq.(22) the blocks are:

$$\begin{aligned} \mathcal{Q}_n &= i\omega + \hat{\mathcal{L}}_S + \hat{\mathcal{L}}_{SV} - n\Lambda\hat{1} \\ \mathcal{Q}_n^- &= \frac{1}{\sqrt{2}}\hat{\mathcal{L}}_{QS} \\ \mathcal{Q}_n^+ &= \sqrt{2}(n+1)\hat{\mathcal{L}}_{QS} \end{aligned}$$

The SLE may be solved in the frequency-domain using a matrix continued fraction<sup>15,27,29</sup> The Green's function is given by the inverse (Eq.24) of the tridiagonal matrix Eq.(E1). Starting with

$$\left[ i\omega + \hat{\mathcal{L}} \right] \mathcal{G}(\omega) = -\hat{1}$$

For the off- diagonal  $n \neq m$  elements we have

$$\mathcal{Q}_n^- \mathcal{G}_{n-1,m} + \mathcal{Q}_n \mathcal{G}_{n,m} + \mathcal{Q}_n^+ \mathcal{G}_{n+1,m} = 0 \quad (\text{E2})$$

The diagonal  $n = m$  elements are

$$\mathcal{Q}_n^- \mathcal{G}_{n-1,n} + \mathcal{Q}_n \mathcal{G}_{n,n} + \mathcal{Q}_n^+ \mathcal{G}_{n+1,n} = -1 \quad (\text{E3})$$

The recursion relation Eq. (E2) is independent of the index  $m$ . Consequently we can introduce the matrices  $\mathcal{S}^+, \mathcal{S}^-$

$$\mathcal{G}_{n\pm 1,b} = \mathcal{S}_n^\pm \mathcal{G}_{n,m} \quad (\text{E4})$$

Using Eq. (E2) these matrices may be solved iteratively.

$$\mathcal{S}_n^\pm = \frac{-1}{\mathcal{Q}_{n\pm 1} + \mathcal{Q}_{n\pm 1}^\pm \mathcal{S}_{n\pm 1}^\pm} \mathcal{Q}_{n\pm 1}^\mp \quad (\text{E5})$$

Combined with Eq. (E3) we obtain for the diagonal terms:

$$\mathcal{G}_{n,n} = \frac{-1}{\mathcal{Q}_n^- \mathcal{S}_n^- + \mathcal{Q}_n + \mathcal{Q}_n^+ \mathcal{S}_n^+} \quad (\text{E6})$$

while the off-diagonal  $\mathcal{G}(\omega)_{nm}$  are obtained from Eq.(E5) and (E4). For  $n > m$

$$\mathcal{G}_{n,m}(\omega) = \mathcal{S}_{n-1}^+(\omega) \mathcal{S}_{n-2}^+(\omega) \cdots \mathcal{S}_m^+(\omega) \mathcal{G}_{m,m}(\omega) \quad (\text{E7})$$

and for  $n < m$

$$\mathcal{G}_{n,m}(\omega) = \mathcal{S}_{n+1}^-(\omega) \mathcal{S}_{n+2}^-(\omega) \cdots \mathcal{S}_m^-(\omega) \mathcal{G}_{m,m}(\omega) \quad (\text{E8})$$

The full Green's function  $\mathcal{G}(\omega)$  can be calculated by using Eq. (E5) to find the connection matrices  $\mathcal{S}^\pm$ . We note that  $\mathcal{S}_0^-$  is zero and truncate the recurrence relation for  $\mathcal{S}^+$  at some

level  $n$  by setting  $\mathcal{S}_n^+$  equal to zero. The matrix elements  $\mathcal{G}(\omega)_{mm}$  can then be obtained using Eq. (E6). All other matrix elements  $\mathcal{G}(\omega)_{nm}$  are calculated from Eq. (E4).

- 
- <sup>1</sup> J. Zheng, K. Kwak, J. Asbury, X. Chen, I. R. Piletic, and M. D. Fayer, *Science* **309**, 1338 (2005).
  - <sup>2</sup> J. Asbury, T. Steinel, and M. D. Fayer, *J. Lum* **107**, 271 (2004).
  - <sup>3</sup> Y. S. Kim and R. M. Hochstrasser, *PNAS* **102**,1185 (2005).
  - <sup>4</sup> S. Mukamel, *Annu. Rev. Phys. Chem.* **51**, 691 (2000).
  - <sup>5</sup> D. M. Jonas, *Annu. Phys. Rev. Chem.* **54**, 425 (2003).
  - <sup>6</sup> Chem Phys. Special Issue: Multidimensional Spectroscopy Vol 266, No 2 ,3, edited by S. Mukamel and R. M. Hochstrasser.
  - <sup>7</sup> R. Kubo "A stochastic theory of line-shape and relaxation". in: *Flucutation, relaxation and resonance in magnetic systems*, D. ter Haar, Ed. Oliver & Boyd ,Edinburgh, 1962,p.23.
  - <sup>8</sup> R. R. Ernst , G.Bodenhausen,and A.Wokaun,*Principles of Nuclear Magnetic Resonance in One nad Two Dimensions*, (Oxford University Press, New York, 1987).
  - <sup>9</sup> B. H. Meier and R. R. Ernst, *J. Am. Chem. Soc.* **101**, 6441 (1979).
  - <sup>10</sup> D. Gamliel and H. Levanon *Stochastic processes in Magnetic Resonance* (World Scientific,1995).
  - <sup>11</sup> N. G. van Kampen, *Stochastic processes in Physics and Chemistry*, (North Holland, Amsterdam, 1992).
  - <sup>12</sup> S.N.Vinogradov and R. H. Linell, *Hydrogen bonding*(von Nostrand Reinhold, New York, 1971).
  - <sup>13</sup> *The Hydrogen Bond: Recent Developments in Theory and Experiments* edited by P. Schuster, G. Zundel, and C. Sandorfy (North-Holland, Amsterdam, 1976).
  - <sup>14</sup> *Ultrafast Hydrogen Bonding Dynamics and Proton Transfer Processes in the Condenced Phase*, edited by T. Elsaesser and H. J. Bakker (Kluwer Academic, Dordrecht, 2002).
  - <sup>15</sup> T. I. C. Jansen, W. Zhuang, and S. Mukamel, *J. Chem. Phys.* **121**, 10577 (2004).
  - <sup>16</sup> T. I. C. Jansen, T. Hayashi, W. Zhuang, and S. Mukamel, *J. Chem. Phys.* **123**, 114504 (2005).
  - <sup>17</sup> R. Kubo, *J. Math. Phys.* **4**, 174 (1963).
  - <sup>18</sup> P. W. Anderson, B. I. Halperin, and C. M. Varma, *Philos. Mag.* **25**, 1 (1971).
  - <sup>19</sup> Y. Zhao, V. Chernyak, and S. Mukamel, *J. Phys. Chem A* **102**, 6614 (1998).
  - <sup>20</sup> F. Šanda and S. Mukamel, *Phys. Rev. E* **73** 011108 (2006).

- <sup>21</sup> A. O. Caldeira and A.J.Leggett, *Physica A* **121**, 587 (1983).
- <sup>22</sup> C. Cohen-Tanoudji, J. Dupon-Roc, and G. Grynberg, *Atom Photon Interaction* (Wiley, New York, 1957).
- <sup>23</sup> S. Mukamel, *Principles of Nonlinear Optical Spectroscopy*, (Oxford University Press, New York, 1995).
- <sup>24</sup> Ch. Scheurer and S. Mukamel, *J. Chem. Phys.* **115**, 4989 (2001) .
- <sup>25</sup> M. Khalil, N. Demirdöven, A. Tokmakoff, *Phys. Rev. Lett* **90**,047401 (2003).
- <sup>26</sup> R. Kubo, M. Toda, and N. Hashitsume, *Statistical Physics II*, (Springer, Berlin,1995).
- <sup>27</sup> H. Risken, *The Fokker-Planck Equation*, (Springer, Berlin,1989).
- <sup>28</sup> Y. Tanimura and T. Steffen, *J. Phys. Soc. Jpn.* **69**, **4095** (2000).
- <sup>29</sup> Y. Tanimura and R. Kubo: *J. Phys. Soc. Jpn.* **58** 101 (1989) 101.
- <sup>30</sup> K. Okomura, A. Tokmakoff, Y. Tanimura, *Chem. Phys. Lett.* **314**, 488 (1999).
- <sup>31</sup> Y. J. Yan, and S. Mukamel, *J. Chem. Phys* **89**, 5160 (1988).
- <sup>32</sup> J. J. Markham, *Rev. Mod. Phys.* **31** 965 (1959).
- <sup>33</sup> S. Mukamel, *Phys Rev. A* **28**, 3480 (1983).
- <sup>34</sup> D. Abramavicius and S. Mukamel, *Chem. Rev.* **104**, 2073 (2004).
- <sup>35</sup> R. Venkatramani; S. Mukamel, *J. Chem. Phys.***117**, 11089 (2002).
- <sup>36</sup> T. Meier, V. Chernyak, and S. Mukamel,*J. Chem. Phys.***107**, 8759 (1997).

## Figure captions

Fig 1 Top: Pulse configuration for a three pulse coherent experiment

Bottom: Feynman diagrams for the third order coherent response of an anharmonic vibrations. The diagrams correspond respectively to the six terms in Eq. (6).

Fig 2 (Color Online) 2D signals  $S_A$  (Eq.(10)) for the TSJ model (Eqs. (14), (10)), (a), static limit  $\Omega_1/k_u = 5$  for short delay  $k_u t_2 = 0$ ,  $\Delta_0 = -4\Omega_1$ ,  $k_d = k_u$ ,  $\Delta_1 = 0$ .

(b), static limit  $\Omega_1/k_u = 5$ , for long delay  $k_u t_2 = 2.0$ ,  $\Delta_0 = -4\Omega_1$ ,  $k_d = k_u$ ,  $\Delta_1 = 0$

(c), fast chemical exchange (motional narrowing)  $\Omega_1/k_u = 0.2$ ,  $\Delta_0 = -4\Omega_1$ ,  $\Delta_1 = 0$ ,  $k_d = k_u$ ,  $k_u t_2 = 0$ .

Fig 3 (Color online) The 2D signal  $S_A$  signal (Eqs.(10)) including TSJ and the fast spectral diffusion:  $\Omega_2/\Lambda = 0.2$ ;  $\Omega_2/\Omega_1 = 3$ ,  $k_d = k_u = 0.002\Omega_1$ ;  $\Delta_0 = -4\Omega_1$ ,  $\Omega_3 = \Delta_3 = \Delta_1 = \Delta_2 = 0$ ;

(a)  $k_d t_2 = 0$ ; (b)  $k_d t_2 = 1$ .

Fig 4 (Color online) The 2D  $S_A$  signal (Eqs.(10)). with TSJ and slow spectral diffusion.  $\Omega_2/\Lambda = 5$ ,  $\Omega_2/\Omega_1 = 0.5$ ,  $k_d = k_u = 0.002\Omega_1$ ,  $\Delta_0 = -4\Omega_1$ ,  $\Omega_3 = \Delta_3 = \Delta_2 = \Delta_1 = 0$ ;

at times a,  $\Lambda t_2 = 0$ ; b,  $\Lambda t_2 = 5$  (i.e.  $k_d t_2 = 0.1$ ) c,  $k_d t_2 = 1$ .

Fig 5 (Color online) 2D signals for  $S_I$  generated along  $\mathbf{k}_I$  (Eq. (8)), and  $S_{II}$  generated along  $\mathbf{k}_{II}$  (Eq. 9)

(a)  $k_{II}$ ,  $\Lambda t_2 = 0$

(b)  $k_I$ ,  $\Lambda t_2 = 0$

(c)  $k_{II}$ ,  $\Lambda t_2 = 5$

(d)  $k_I$ ,  $\Lambda t_2 = 5$

Other parameters same as in Fig 4.

Fig 6 (Color online) 2D signal  $S_A$  (Eqs.(10)) with spectral diffusion and TSJ. Spectral diffusion linewidth is varied ( $\Delta_2 \neq 0$ ). Slow spectral diffusion in *eg* state, fast diffusion in overtone *ef*:  $\Omega_2/\Lambda = 2$ ,  $\Omega_2/\Omega_1 = 0.6$ ,  $k_d = k_u = 0.002\Omega_1$ ,  $\Delta_0 = -4\Omega_1$ ,  $\Delta_2 = -0.75\Omega_2$ ,  $\Omega_3 = \Delta_3 = \Delta_1 = 0$ ;

(a)  $\Lambda t_2 = 0$ ; (b)  $\Lambda t_2 = 15$  (i.e.  $k_d t_2 = 0.1$ ); (c)  $k_d t_2 = 1$ .

Fig 7 (Color online) Absorption lineshape for our model Eq.(22) with different spectral diffusion width in the  $u$  and  $d$  states ( $\Omega_3 \neq 0$ ).  $\Omega_1 = 0.5fs^{-1}$   $\Lambda = 0.4ps^{-1}$ ;  $\Omega_2 = 0.33ps^{-1}$ ,  $\Omega_3 = -0.07ps^{-1}$   $k_d = 0.125ps^{-1}$ ,  $k_u = 0.1ps$ ,  $\Delta_0 = -2.0ps^{-1}$ ,  $\Delta_2 = 0$ ,  $\Delta_3 = \Delta_1 = 0$ ;

Fig 8 (Color online) The 2D signal  $S_A$  (Eq. 10) for the same parameters of Fig 7 at various time delays (a)  $t_2 = 0$ ; (b)  $t_2 = 2ps$ ; (c)  $t_2 = 10ps$ . These spectra close resemble the experimental result of<sup>1</sup>.

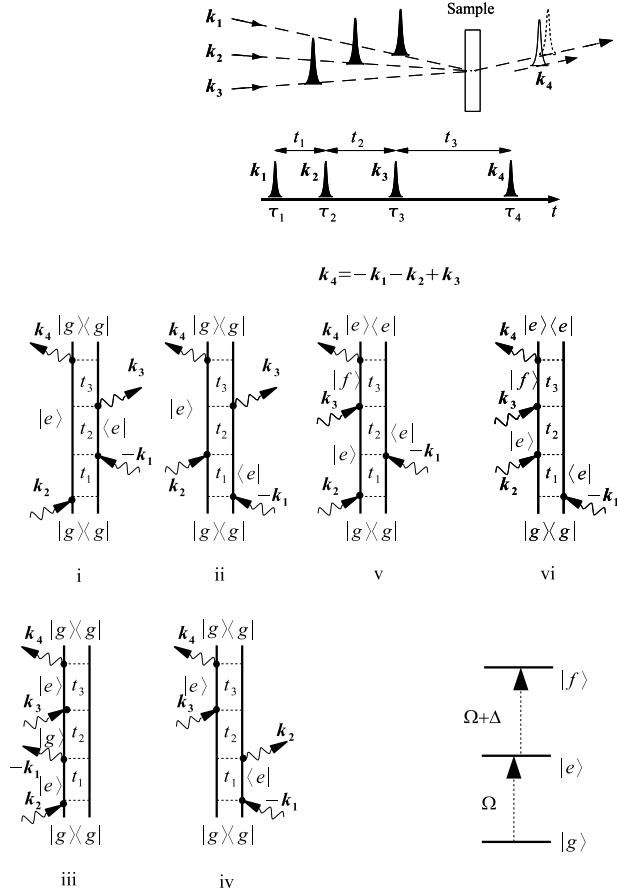
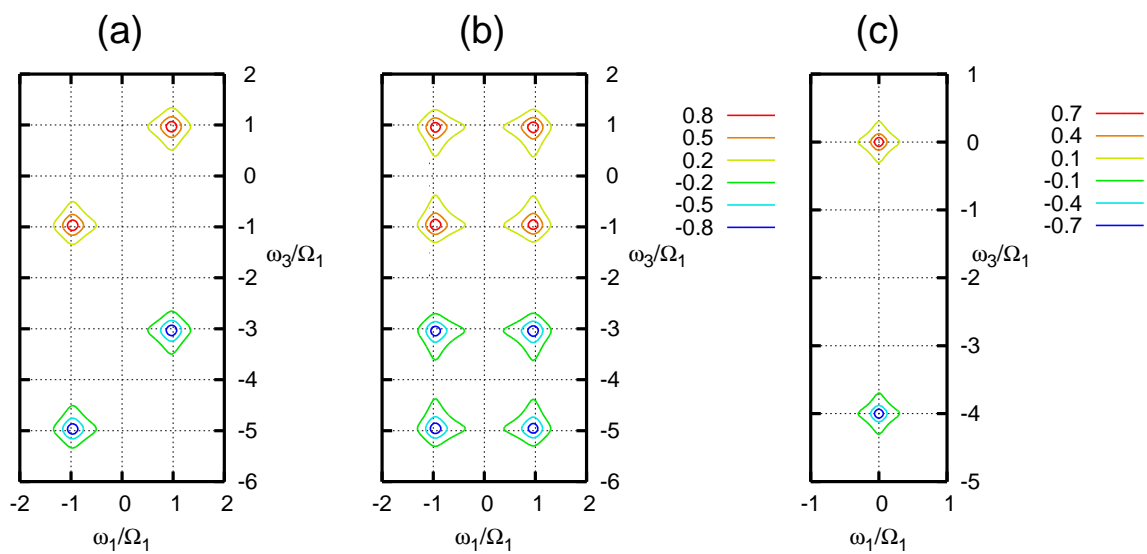
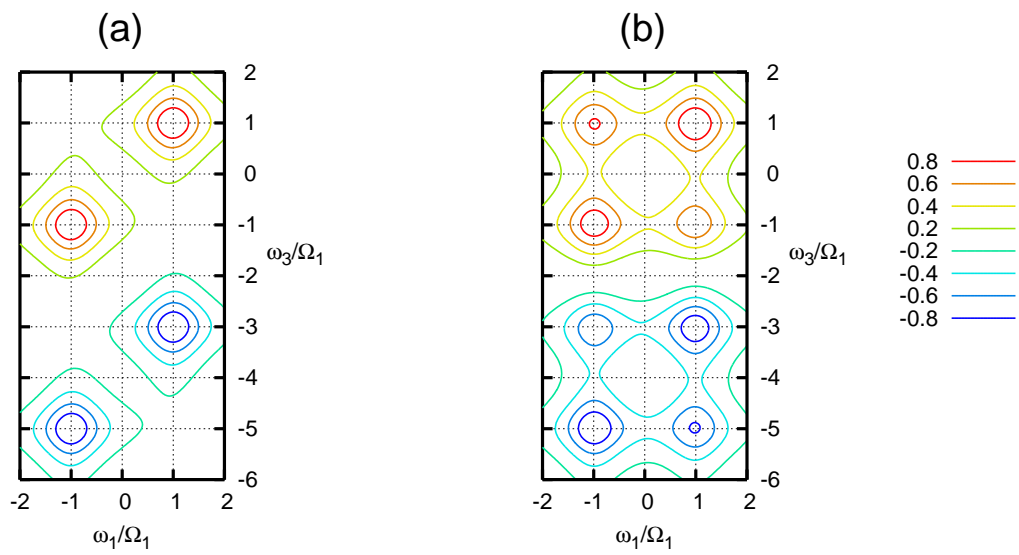


Fig 1



**Fig 2**





**Fig 3**

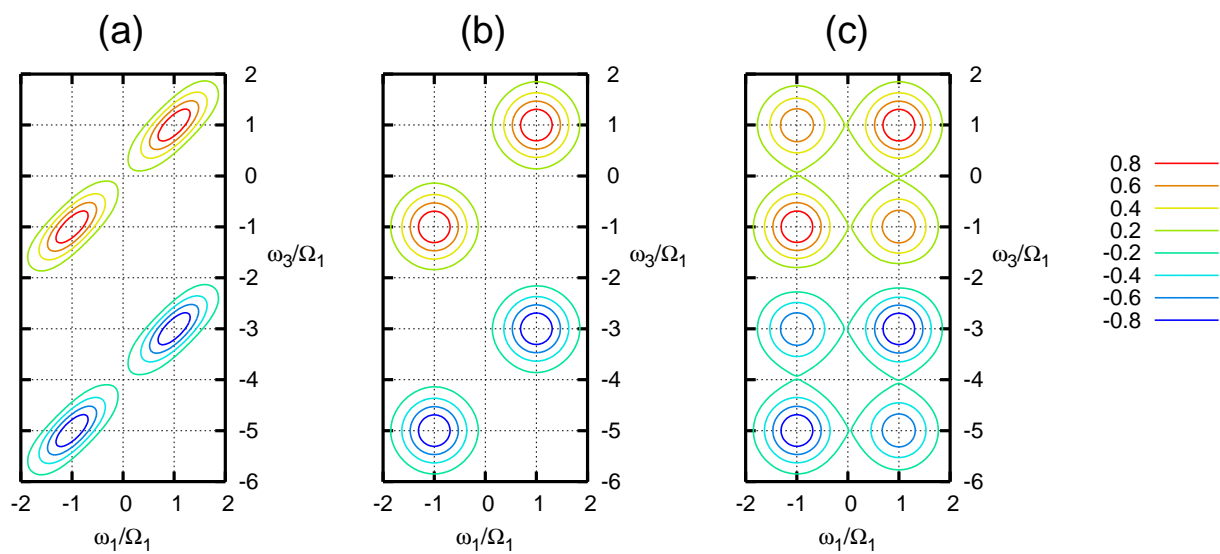
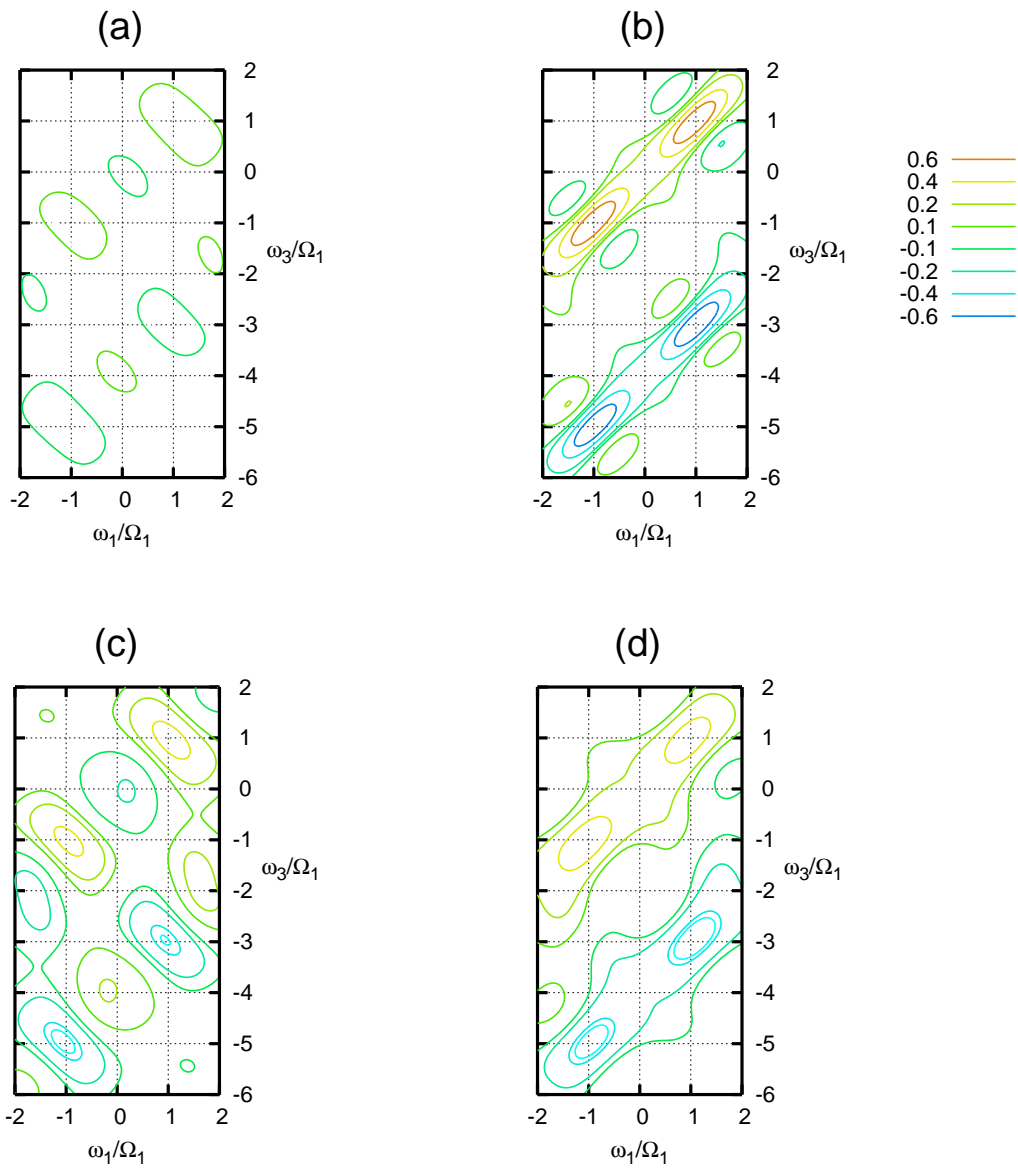


Fig 4



**Fig 5**

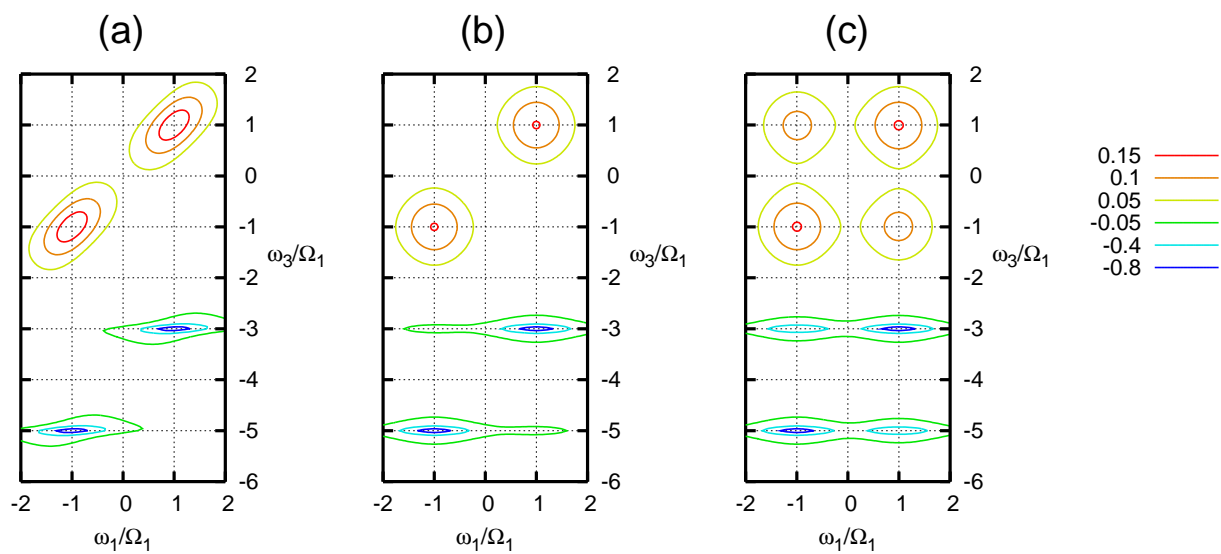
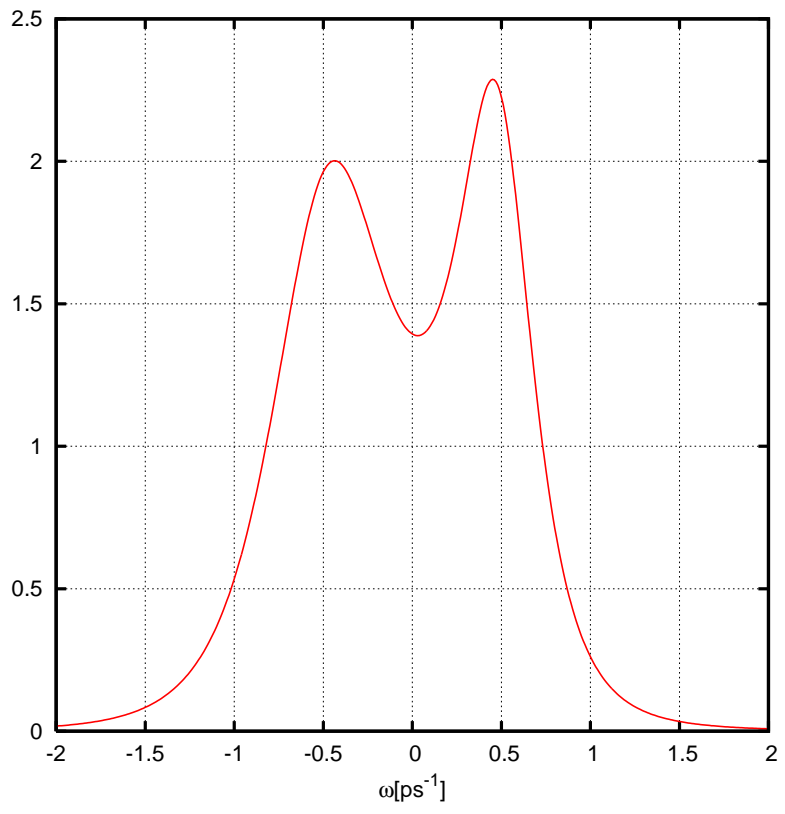
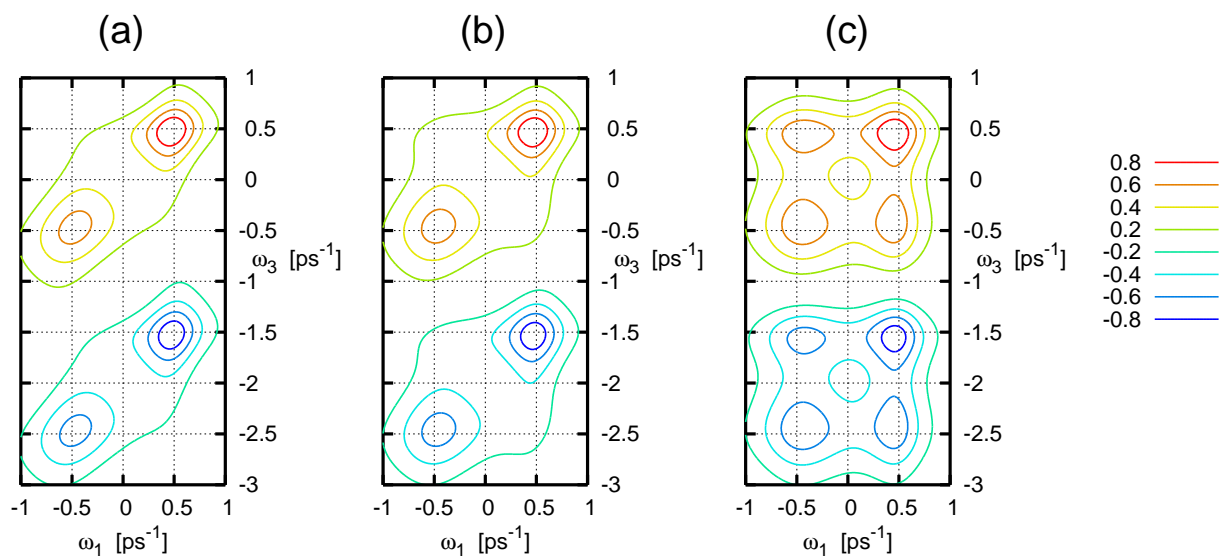


Fig 6



**Fig 7**



**Fig 8**